



# CERTIFICATE of participation

IS PRESENTED TO



*Bilal Djamel Eddine CHERIF*

Title : **Diagnosis of Induction Motor Bearing Fault Using the  
Vibration Signal Processing**

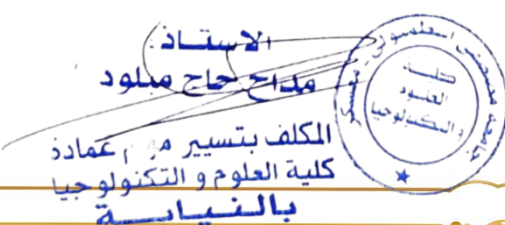
In the **1<sup>st</sup> National Conference on Emerging Trends in Engineering and  
Technology (NC2ET'25)**

Faculty of Sciences and Technology, Mustapha Stambouli University  
Mascara, Algeria  
April 22<sup>th</sup> - 23<sup>th</sup>, 2025

Co-authored-by : Sara SENINETE, Hilal RAHALI



Paper ID:202





## Participation Form

**Authors:** Bilal Djamel Eddine CHERIF, Sara SENINETE, Hilal RAHALI

**Manuscript Title:** Diagnosis of Induction Motor Bearing Fault Using the Vibration Signal Processing.

**E-mail:** [cherif.bilaldjamaleddine@univ-msila.dz](mailto:cherif.bilaldjamaleddine@univ-msila.dz), [saraseninete@gmail.com](mailto:saraseninete@gmail.com),  
[hilal.rahali@univ-msila.dz](mailto:hilal.rahali@univ-msila.dz)

**Company Name:** Electrical Engineering Laboratory (LGE), Department of Electrical Engineering, Faculty of Technology, University of M'sila, University Pole, Road Bourdj Bou Arreridj, M'sila 28000.

### Manuscript Topic:

**Topic 1:** Electrical Power Components and Systems

**Topic 2:** Renewable Energies

**Topic 3:** Electromechanics

**Topic 4:** Electrical Machines

**Topic 5:** Automation & Control

**Topic 6:** Electronics and Computer Engineering

**Topic 7:** Telecommunication systems

**Topic 8:** Signal, Image and Video Processing

X

**Participant Name:** Bilal Djamel Eddine CHERIF

<b>Participation Type:</b>	Onsite	<input type="checkbox"/>	Online	<input type="checkbox"/>
<b>Presentation Type:</b>	Oral	<input type="checkbox"/>	Poster	<input checked="" type="checkbox"/>



# Diagnosis of Induction Motor Bearing Fault Using the Vibration Signal Processing

Bilal Djamel Eddine Cherif<sup>\*1</sup>, Sara Seninete<sup>2</sup> and Hilal Rahali<sup>1</sup>

<sup>1</sup> Electrical Engineering Laboratory (LGE), Department of Electrical Engineering, Faculty of Technology, University of M'sila, University Pole, Road Bourdj Bou Arreridj, M'sila 28000

<sup>2</sup> Department of Electrical Engineering, Faculty of Technology, University of Mostaganem, Mostaganem 27000

<sup>\*</sup>cherif.bilaldjamaleddine@univ-msila.dz

## Keywords:

Bearing  
Fault  
Outer race  
Inner race  
Rolling elements  
DWT

**Abstract** – In this paper, we propose a diagnostic method for detecting and localizing bearing faults in induction motors using a combination of discrete wavelet transforms (DWT) and the spectral envelope derived from the Hilbert transform. The DWT is used to extract the detail coefficients, while the Hilbert transform is employed to compute the temporal envelope and the envelope spectrum of the reconstructed signal from the relevant detail coefficients. The Kurtosis value is used to determine the optimal wavelet decomposition level containing the key fault-related frequencies, enabling early fault detection and localization. The proposed approach is validated using the Sheen model, which generates the vibration signal for analysis.

## I. INTRODUCTION

Induction motors are essential in industrial applications, but their malfunctions can lead to production disruptions and increased maintenance costs. Statistical studies indicate that the majority of faults in rotating machines are associated with bearing failures. Predicting these failures can significantly reduce maintenance expenses, including motor downtime, spare parts consumption, and overall operational inefficiencies [1].

Bearing monitoring is crucial for ensuring the reliability and operational safety of induction motors. It primarily involves extracting information that reveals signs of degradation. Various physical parameters are used for this purpose, including electrical currents, pressure, oil analysis, temperature monitoring, acoustic emissions, and vibration analysis, all of which help assess the condition of the bearings [2].

Vibration analysis is the most widely used technique for monitoring and diagnosing bearing defects. During operation, a bearing generates complex vibration signals, which are captured by accelerometers placed on the bearings of rotating machines and recorded using a data acquisition system. Vibration analysis is conducted at three levels [3, 4]:

- **Monitoring:** Utilizes global indicators to characterize changes in bearing behavior;
- **Diagnosis:** Employs signal processing tools to identify and locate defects;
- **Follow-up:** Tracks the progression of damage in defective components to assess their condition over time.

Various studies have been conducted using wavelet theory to overcome the limitations of traditional analysis techniques. Wavelet analysis is a modern signal processing method that has been widely applied in fault detection and remains an active area of research across multiple fields. While it offers significant advantages, it also comes with certain limitations [5, 6].

The advantages:

**Multi-Scale Representation:** Wavelets enable the representation of a signal or image at multiple scales, facilitating a more detailed analysis of local features and variations;

**Precise Localization:** Wavelets offer accurate localization in both the time and frequency domains, enabling the precise identification of changes and transitions within a signal;

**Efficient Compression:** Wavelets are extensively used in data compression as they enable a more compact representation of signals by removing non-essential details, reducing storage and transmission requirements;

**Anomaly Detection:** Wavelet methods excel at detecting anomalies or irregularities in signals by emphasizing significant variations and deviations, making them highly effective for fault detection and error analysis;

**Adaptability to Complex Structures:** Wavelets are well-suited for analyzing signals with intricate structures, including non-stationary signals and those with discontinuities, making them highly versatile for various signal processing applications. The limitations:

**Selecting the Appropriate Wavelet Function:** Choosing the right wavelet function can be challenging, as it must be tailored to the specific characteristics of the signal being analyzed;

**Selection of Decomposition Parameters:** Wavelet methods require careful selection of decomposition parameters, such as the decomposition level and compression thresholds. This process can be iterative and somewhat subjective, impacting the accuracy and effectiveness of the analysis;

**Computational Complexity:** Performing a wavelet transform can be computationally intensive, requiring significant processing time and resources, especially for high-resolution signals or real-time applications;

**Interpretation of Coefficients:** Analyzing wavelet coefficients can be challenging, as they may contain both useful signal features and unwanted noise. Proper interpretation requires expertise to distinguish meaningful patterns from irrelevant variations.

It's important to acknowledge that the advantages and disadvantages of wavelet methods can vary depending on the specific application and the problem at hand. As such, careful consideration of these factors is crucial when selecting and implementing wavelet techniques.

We will not elaborate further on this technique here, as its concept, mathematical foundations, and properties will be thoroughly explained in the following sections of this paper.

The remainder of the paper is structured as follows: Section 2 provides a brief overview of the characteristic frequencies associated with a faulty bearing. Section 3 introduces the Sheen model used to generate the vibration signal analyzed in this study. In Section 4, we elaborate on the method employed for fault detection and localization of faulty components within the bearing. Finally, the paper concludes with a summary and discussion in the conclusion section.

## II. OVERVIEW OF FREQUENCIES ASSOCIATED WITH BEARING FAULTS

The characteristic fault frequencies of a bearing are defined by its geometry, as illustrated in Fig. 1.

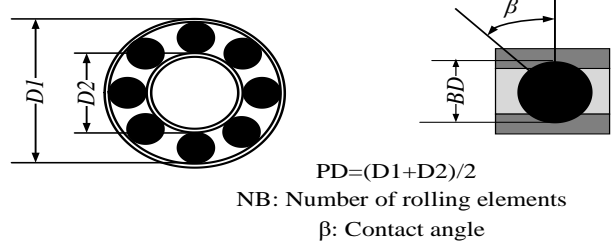


Fig. 1 Characteristic of bearing [7]

The characteristic frequency for an outer-race fault is expressed by equation (1) [8]:

$$f_{or} = \frac{N_b}{2} f_r \left[ 1 - \frac{B_D}{P_D} \cos \beta \right] \quad (1)$$

The characteristic frequency for an inner-race fault is expressed by equation (2) [8]:

$$f_{ir} = \frac{N_b}{2} f_r \left[ 1 + \frac{B_D}{P_D} \cos \beta \right] \quad (2)$$

The characteristic frequency for a rolling elements fault is expressed by equation (3) [8]:

$$f_{re} = \frac{P_D}{B_D} f_r \left[ 1 + \left( \frac{B_D}{P_D} \cos \beta \right)^2 \right] \quad (3)$$

Where:  $N_b$ : number of rolling elements bearings,  $P_D$ : intermediate diameter,  $B_D$ : diameter of rolling elements bearings,  $\beta$ : contact angle,  $f_r$ : rotation frequency.

## III. SHEEN MODEL

The complex filter can be represented in the following form [9]:

$$h(t) = h_r(t) + jh_i(t) \quad (4)$$

In the following, a complex filter for the Hilbert transform is proposed and defined as [9]:

$$h_{a,f_c,f_\omega}(t) = \frac{1}{j\pi t} e^{-(t/a)^2} \left( e^{-j2\pi(f_c - f_\omega/2)t} - e^{-j2\pi(f_c + f_\omega/2)t} \right) \quad (5)$$

$h_r(t)$  and  $h_i(t)$ , respectively, can be expressed as follows:

$$h_r(t) = \frac{1}{\pi t} e^{-(t/a)^2} \left[ \sin\left(2\pi\left(f_c + \frac{f_\omega}{2}\right)t\right) - \sin\left(2\pi\left(f_c - \frac{f_\omega}{2}\right)t\right) \right] \quad (6)$$

$$h_r(t) = \frac{1}{\pi t} e^{-(t/a)^2} \left[ \cos\left(2\pi\left(f_c + \frac{f_\omega}{2}\right)t\right) - \cos\left(2\pi\left(f_c - \frac{f_\omega}{2}\right)t\right) \right] \quad (7)$$

Where:  $a$ : represents the scale factor and  $f_c, f_\omega$ : The center frequency and bandwidth, respectively.

The extraction of vibration signal information is achieved through demodulation [9]:

$$x(k) = e^{-\alpha k t} (\sin 2\pi f_1 k T_s) + (\sin 2\pi f_2 k T_s) + (\sin 2\pi f_3 k T_s) \quad (8)$$

$$t' = \text{mod}\left(k T_s, \frac{1}{f_0}\right) \quad (9)$$

This implies that  $e^{-\alpha k t'}$  serves as the modulating signal, while  $\sin(2\pi f_1 k T_s) + \sin(2\pi f_2 k T_s)$  functions as the carrier signal.

Where:  $f_1$  and  $f_2$  are the resonance frequencies;  $f_0$  is the impact fault frequency;  $\alpha$  is the exponential frequency;  $k$  is the number of iterations;  $T_s$  is the sampling time.

Bearing fault signals are simulated using parameters derived from real measurements obtained from the *CWRU* test bench.

The specific traits observed using the *CWRU* (Case Western Reserve University) test bench are as follows [10]:

The bearing operates under a load of 12.3 Nm, with a rotational speed of 1730 rpm. The data is captured at a sampling frequency of 12,000 Hz, corresponding to a defect diameter of 0.1778 mm.

The rotational frequency is  $f_r=28.83$  Hz while the fault frequencies are as follows: the outer race fault frequency is  $f_{or}=103.12$  Hz, the rolling elements fault frequency is  $f_{re}=146.46$  Hz, and the inner race fault frequency is  $f_{ir}=156.34$  Hz.

#### IV. APPLICATION OF DISCRETE WAVELET-BASED SIGNAL PROCESSING METHOD TO BEARING FAULT DETECTION

The proposed methodology consists of the following steps:

**Step 1:** Determine the decomposition level;

**Step 2:** Perform multiresolution wavelet analysis on the signal up to  $n$  levels using the Haar wavelet.

**Step 3:** Calculate the correlation coefficients between the original signal and its detail components;

**Step 4:** Identify detail components with correlation coefficients greater than 0.2 as significant modes;

**Step 5:** Reconstruct the signal by summing the filtered detail components;

**Step 6:** Calculate the kurtosis of the reconstructed signal to identify the presence of defects;

**Step 7:** Apply envelope analysis to determine the location of the defect, if present.

##### A. DWT Transform

The discrete wavelet transform (DWT) employs discretized scale and translation factors, where the parameters are represented as  $a$  and  $b$  [11].

$$\begin{cases} a = a_0^m \\ b = nb_0 a_0^m \end{cases} \quad (10)$$

Where:  $a_0$  is a dilation parameter and  $b_0$  is a translation parameter.

For the majority of applications we choose  $a_0 = 2$  and  $b_0 = 1$ . The translation step  $b = nb_0 2^m$  which corresponds to a dynamic network  $(t, f) = (nb_0 2^m, 2^m f_0)$  where  $f_0$  the frequency of the mother wavelet [12]:

$$\psi_{m,n}(t) = a_0^{\frac{m}{2}} \psi\left(a_0^{-m}t - nb_0\right) \quad (11)$$

##### B. Haar Wavelet

Haar introduced a function  $y(t)$ , which is defined by the following equation [13]:

$$\psi(t) = \begin{cases} 1 & \text{for } 0 \leq t \leq \frac{1}{2} \\ -1 & \text{for } \frac{1}{2} \leq t \leq 1 \\ 0 & \text{ailleurs} \end{cases} \quad (12)$$

##### C. Number of Calculation Levels for Decomposition

Choice of the optimal number of decomposition levels: The levels of vibration signals decomposition are expressed by the following equation [14]:

$$n = 1.44 \log\left(\frac{F_{\max}}{3F_c}\right) \quad (13)$$

Where:  $n$  is an integer rounded up,  $F_c$  is a shock frequency and  $F_{max}$  is the maximum frequency of the signal.

## V. STATISTICAL FACTORS

This section examines the statistical factors Correlation coefficient (*Corr*) and Kurtosis (*Ku*) for each detail.

### A. *Corr*

The *Corr* is a crucial tool for selecting appropriate modes in a given time series, as determined by the equation [15]:

$$Corr(i) = \sum_{t=1}^L \frac{x(t)d_i(t)}{\sqrt{\sum_{t=1}^L x^2(t)} \sqrt{\sum_{t=1}^L d_i^2(t)}} \quad (14)$$

### B. *Ku*

It quantifies the degree of flattening in the distribution, offering insight into the prominence of the peak at the curve's apex. It is defined as [16]:

$$K_u = \frac{1}{N} \sum_{i=1}^N \left[ \frac{x_i - \bar{x}}{\sigma} \right]^4. \quad (15)$$

When a bearing is in optimal condition, the distribution of the collected signal amplitudes follows a Gaussian distribution, resulting in a Kurtosis value close to 3. However, the occurrence of a defect causes the Kurtosis value to rise above 3.

## VI. ENVELOPE SPECTRAL ANALYSIS

The spectral envelope is defined using the following equations [17]:

$$\overline{DSR} = \frac{1}{\pi} \int \frac{DSR(\tau)}{t - \tau} dt \quad (16)$$

$$\overline{DSR} = DSR(t) + j\overline{DSR(t)} \quad (17)$$

$$|DSR(t)| = \sqrt{DSR(t)^2 + \overline{DSR(t)}^2} \quad (18)$$

## VII. SIMULATION RESULTS AND INTERPRETATION

Fig. 2, illustrates the vibration signals for both healthy and faulty conditions, clearly emphasizing the distinct patterns linked to outer race, rolling element, and inner race faults.

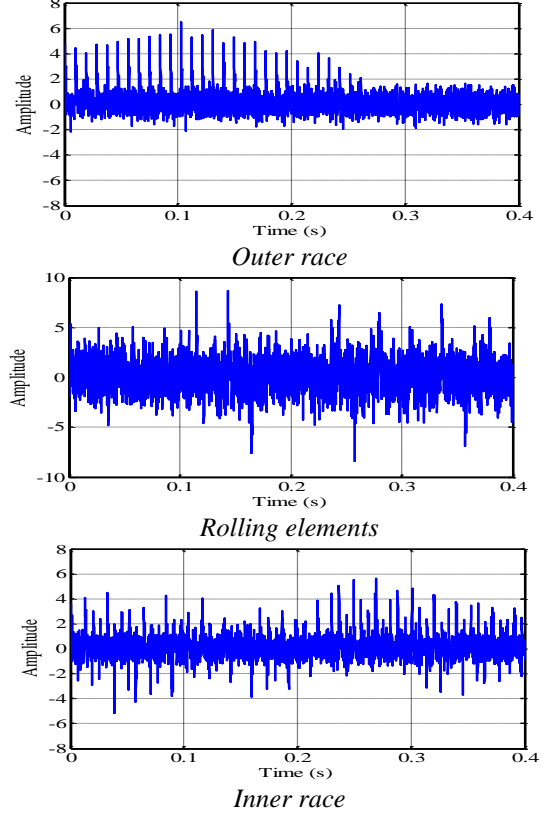


Fig. 2 Vibration signals

From Equation (9), the number of Haar wavelet decomposition levels is determined to be  $n=7$ .

Fig. 3, illustrates the correlation coefficients corresponding to outer race, rolling elements, and inner race fault.

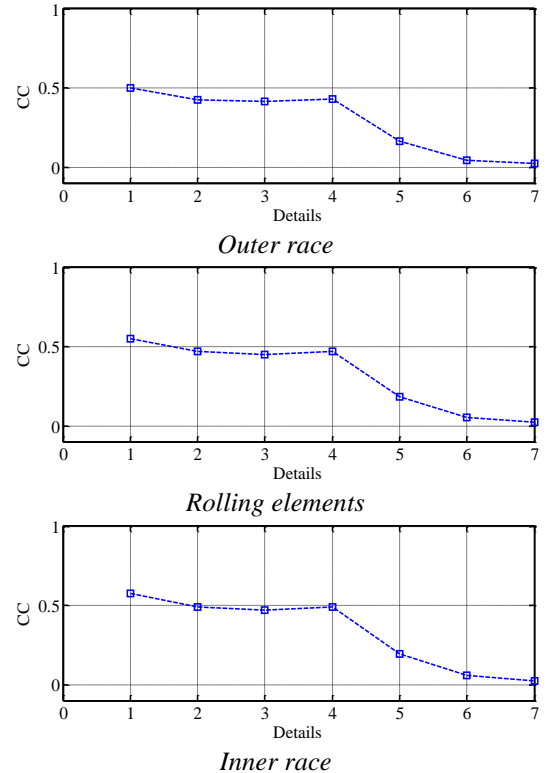


Fig. 3 Correlation coefficients

Fig. 3, illustrates the correlation coefficients between the original signals and their corresponding details. The details with correlation coefficients exceeding the threshold, where the average correlation coefficient is 0.2, are highlighted.

Table 1 presents the details that are useful for each case.

Table 1. Useful details

Case	Outer race	Rolling elements	Inner race
Details	$d_1, d_2, d_3$ and $d_4$	$d_1, d_2, d_3$ and $d_4$	$d_1, d_2, d_3$ and $d_4$

Fig. 4, depicts both the original signal and the filtered signal.

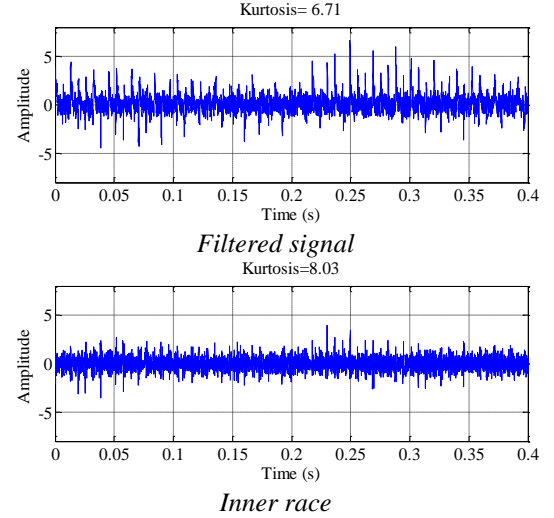
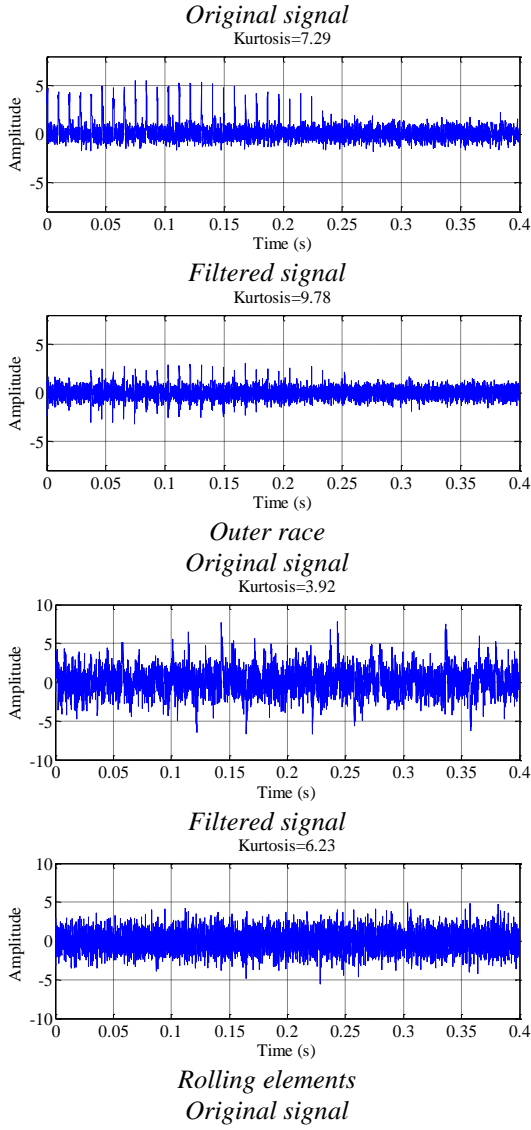


Fig. 4 Original signal and filtered signal

It is observed that the Kurtosis value increases after filtering the vibration signal in all fault cases. For an outer race fault, the Kurtosis value rises from 7.29 before filtering to 9.78 after filtering. Similarly, in the case of a rolling elements fault, the value increases from 3.92 to 6.23, and for an inner race fault, it grows from 6.71 before filtering to 8.03 after filtering.

Fig.5, illustrates the spectral envelope of the filtered signal for the outer race, rolling elements, and inner race fault.

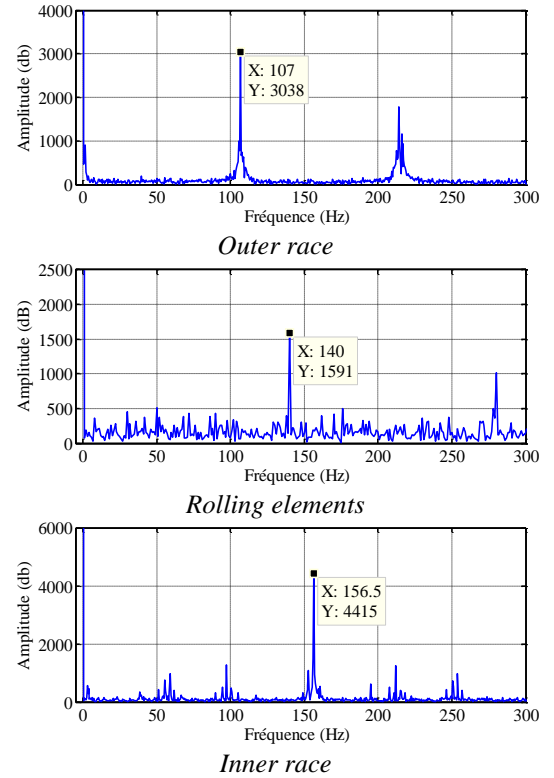


Fig. 5 Spectral envelope

Fig. 5, displays the envelope spectra of the filtered signals, where prominent frequency peaks at 107 Hz, 140 Hz, and 156.5 Hz, along with their

harmonics, are clearly identifiable. These peaks facilitate the identification of faults on the bearing's outer race, rolling elements, and inner race, respectively.

### VIII. CONCLUSION

This paper focuses on diagnosing bearing faults in induction motors using a method based on Discrete Wavelet Transform (DWT). The proposed approach utilizes vibration signal decomposition to identify harmonics that indicate the location of bearing faults. A statistical study is conducted by calculating the correlation coefficient for each detail level. Only details with a correlation coefficient greater than or equal to 0.2 are considered useful, which in this case includes d1, d2, d3, and d4. After reconstructing the useful details, a filtering operation is applied and optimized using the kurtosis factor. An increase in kurtosis confirms the filtering effectiveness before the global signal reconstruction. Finally, spectral envelope analysis is conducted on the reconstructed signal to identify bearing faults. The extracted peaks at 107 Hz, 140 Hz, and 156.5 Hz, along with their harmonics, provide clear indications of faults in different bearing components—the outer race, rolling elements, and inner race, respectively.

The automatic selection of the number of decomposition levels is still a drawback of the DWT, this choice is not optimal for all types of signals. In perspective, the proposed method can be expanded to localize the faulty component using machine learning approaches.

### REFERENCES

- [1] C. B. D. E. S. S and M. D. A novel, machine learning-based feature extraction method for detecting and localizing bearing component defects. *Metrology and Measurement Systems*, 2022, Vol: 29, n=2, pp: 333-346.
- [2] R. Bousseksou. ,N, Bessous., & M. M. Mahmoud. Diagnosis of bearing faults using an advanced feature extraction based on WPT and EEV methods. *Studies in Engineering and Exact Sciences*, 5(2), (2024), e12305-e12305.
- [3] W. H, J. Z, and J. X. *Online bearing fault diagnosis using numerical simulation models and machine learning classifications*. *Reliability Engineering & System Safety* 234 (2023): pp:109142.
- [4] Y. Jiang. The Review of Bearing Fault Diagnosis Technology Based on Machine Learning. *Journal of Advances in Engineering and Technology*, 1(3),(2024), pp : 21-25.
- [5] G. G., and P. G. *An efficient method for bearing fault diagnosis*. *Systems Science & Control Engineering* 12.1 (2024): pp:2329264.
- [6] R. A, et al. *Data Driven Bearing Fault Diagnosis for Induction Motor*. *Journal of Electrical and Computer Engineering* 2023.1 (2023): pp: 7173989.
- [7] Chen, H., Li, S., Lu, X., Zhang, Q., Zhu, J., & Lu, J. Research on bearing fault diagnosis based on a multimodal method. *Mathematical Biosciences and Engineering*, 21(12), (2024), pp : 7688-7706.
- [8] Magadán, L., Ruiz-Cárcel, C., Granda, J. C., Suárez, F. J., & Starr, A. Explainable and interpretable bearing fault classification and diagnosis under limited data. *Advanced Engineering Informatics*, 62, (2024), 102909.
- [9] Peng, C., Sheng, Y., Gui, W., Tang, Z., & Li, C. A rolling bearing fault diagnosis method based on multimodal knowledge graph. *IEEE Transactions on Industrial Informatics*, (2024).
- [10] Khan, M. A., Asad, B., Kudelina, K., Vaimann, T., & Kallaste, A. The bearing faults detection methods for electrical machines—the state of the art. *Energies*, 16(1), (2022), 296.
- [11] Zhang, Q., Yao, Y., Huang, Y., Liu, Y., & Wu, L. A Bearing Fault Diagnosis Model Based on a Simplified Wide Convolutional Neural Network and Random Forrest. *Sensors*, 25(3), (2025), 752.
- [12] Lin, Y.; Huang, S.; Chen, B.; Shi, D.; Zhou, Z.; Deng, R.; Huang, B.; Gu, F.; Ball, A.D. A Novel Drum-Shaped Metastructure Aided Weak Signal Enhancement Method for Bearing Fault Diagnosis. *Mech. Syst. Signal Process.* (2024), 209, 111077.
- [13] Choudhary A., Mian T., and Fatima S., Convolutional neural network based bearing fault diagnosis of rotating machine using thermal images, *Measurement*. (2021) 176,109196, <https://doi.org/10.1016/j.measurem.2021.109196>.
- [14] Fan, H.; Ren, Z.; Zhang, X.; Cao, X.; Ma, H.; Huang, J. A Gray Texture Image Data-Driven Intelligent Fault Diagnosis Method of Induction Motor Rotor-Bearing System under Variable Load Conditions. *Measurement* 2024, 233, 114742.
- [15] Wang, P.; Chen, J. Fault diagnosis of spent fuel shearing machines based on improved residual network. *Ann. Nucl. Energy* 2024, 196, 110228.
- [16] Wang, Y.; Zou, Y.; Hu, W.; Chen, J.; Xiao, Z. Intelligent fault diagnosis of hydroelectric units based on radar maps and improved GoogleNet by depthwise separate convolution. *Meas. Sci. Technol.* 2023, 35, 025103.
- [17] C. B. D. E, et al. *Machine-learning-based diagnosis of an inverter-fed induction motor*. *IEEE Latin America Transactions* 20.6 (2022): pp: 901-911.